Electronic Supplementary Material (ESI) for Journal of Materials Chemistry B.

Supporting Information

Ratiometric imaging of butyrylcholinesterase activity in mice with nonalcoholic fatty liver using AIE-based fluorescent probe

Chunbai Xiang†, [a, b] Jingjing Xiang †, [a] Xing Yang †, [a, b] Chunbin Li, [c] Lihua Zhou, [d] Daoyong Jiang, [a] Yonglin Peng, [e] Zhen Xu, [a] Guanjun Deng, [a] Baode Zhu, [f] Pengfei Zhang* [a] Lintao Cai * [a] and Ping Gong * [a]

a. Guangdong Key Laboratory of Nanomedicine, CAS Key Laboratory of Health Informatics, Shenzhen Bioactive Materials Engineering Lab for Medicine, Institute of Biomedicine and Biotechnology, Shenzhen Institute of Advanced Technology, Chinese Academy of Sciences, Shenzhen 518055, China. *E-mail: pf.zhang@siat.ac.cn, lt.cai@siat.ac.cn and ping.gong@siat.ac.cn.

b. University of Chinese Academy of Sciences, Beijing 100049, China.

c. College of Chemistry and Chemical Engineering, Inner Mongolia University, Hohhot 010021, P. R. China.

d. School of Applied Biology, Shenzhen Institute of Technology, No. 1 Jiangjunmao, Shenzhen 518116, P. R. China.

e. Pinete (Zhongshan) Biotechnology Co., Ltd.

f. School of Chemistry and Environmental Science, Xiangnan University, Chenzhou 423000, China.

†. These authors contributed equally to this work.

*Corresponding authors:
Prof. Ping Gong (ping.gong@siat.ac.cn);
Prof. Lintao Cai (lt.cai@siat.ac.cn);
Dr. Pengfei Zhang (pf.zhang@siat.ac.cn).

Experiment section

Materials

All regents and chemicals were purchased from commercial source and used without further purification. Solvents and other common reagents were obtained from Energy Chemical. Phosphate buffer saline (pH=7.4) was used to prepare all aqueous solutions. Butyrylcholinesterase, acetylcholinesterase, lipase, lysozyme, trypsin, tyrosinase, lactoferrin and pepsine were purchased from Sigma-Aldrich. Human butyrylcholinesterase (BChE) ELISA Kit was purchased from Shanghai MLBIO Biotechnology Co. Ltd (shanghai, China). Other chemicals were purchased from commercial source and used without further purification. Nonalcoholic fatty liver mice (8–10 weeks old) were purchased from Jiangsu ALF Biotechnology Co. Ltd (Jiangsu, China) and all animals received care compliance with the guidelines outlined in the Guide for the Care and Use of Laboratory Animals. The procedures were approved by Shenzhen Institutes of Advanced Technology, Chinese Academy of Sciences Animal Care and Use Committee.

Instruments

^{1}H NMR and ^{13}C NMR spectra were measured on a Bruker ARX 400 MHz spectrometer. High-resolution mass spectra (HRMS) were recorded on a GCT Premier CAB 048 mass spectrometer operating in MALDI-TOF mode. UV-vis absorption spectra were recorded on a Rarian 50 Conc UV-Visible spectrophotometer. Fluorescence emission spectra were recorded on Edinburgh FS5 fluorescence spectrophotometer. Cellular imaging experiments were performed with confocal laser scanning microscope (LSM 900 with Airyscan2, Zeiss, Germany). In vivo imaging was performed on VISQUE® In Vivo Smart-LF imaging system. ELISA was performed on Bio Tek Synergy4. The absolute quantum yield of ER-CE was obtained in PL Quantam Yieled Spectrometer C11347 (HAMAMATSU). HPLC experiments were performed on a liquid chromatograph (UltiMate3000).

Synthesis of TCFIS

2-(3-cyano-4,5,5-trimethyl-5H-furan-2-ylidene) malononitrile (199 mg, 1 mmol), 4-(diethylamino) salicylaldehyde (231 mg, 1.2 mmol) and piperidine (28 μL, 0.6 mmol) was mixed in 15 mL ethanol, The reaction was refluxed overnight, cooled to room temperature, and purified by silica gel chromatography with the mixed solvent of PE/EA (5:1~1:1, v/v) to give TCFIS as a purple solid (325 mg, 85%). ^{1}H NMR (400 MHz, DMSO-d6) δ 10.83 (s, 4H), 8.22 (d, J = 14.7 Hz, 4H), 7.70 (d, J = 9.2 Hz, 4H), 6.94 (d, J = 15.5 Hz, 4H), 6.49 – 6.41 (m, 4H), 6.17 (s, 4H), 4.06 (s, 1H), 4.01 (s, 1H), 3.51 (s, 2H), 1.70 (s, 25H), 1.16 (t, J = 7.0 Hz, 26H). ^{13}C NMR (101 MHz, DMSO-d6) δ 178.02, 175.75, 162.79, 154.55, 114.58, 113.71, 113.35, 112.52, 107.27, 97.69, 96.92, 49.16, 45.04, 39.65, 26.41, 13.15. HRMS(MALDI-TOF): m/z: [M^{+}-H] calcd for $C_{22}H_{21}N_4O_2$: 373.16700; found: 373.16666.

Synthesis of TB-BChE

TCFIS (200 mg, 0.54 mmol), cyclopropanecarboxylic acid chloride (63 mg, 0.6 mmol), and

triethylamine (140 μL, 1 mmol) were dispersed in anhydrous CH_2Cl_2. The reaction was stirred at room temperature for 4 h. The solvent was removed under reduced pressure, and the crude product was purified by with the mixed solvent of PE/EA (5:1~3:1, v/v) to give TB-BChE as a purple solid (210 mg, 82%). ^{1}H NMR (400 MHz, DMSO-d6) δ 8.01 (t, J = 11.0 Hz, 2H), 6.93 (d, J = 15.8 Hz, 1H), 6.76 (d, J = 9.1 Hz, 1H), 6.56 (s, 1H), 3.50 (q, J = 7.2 Hz, 4H), 1.96 (h, J = 5.2, 4.7 Hz, 1H), 1.70 (s, 6H), 1.12 (dt, J = 21.1, 6.7 Hz, 10H). ^{13}C NMR (101 MHz, DMSO-d6) δ 178.15, 175.71, 173.10, 153.83, 153.13, 142.33, 131.58, 114.54, 113.94, 112.91, 110.94, 109.58, 105.82, 98.76, 44.94, 25.71, 13.19, 13.01, 10.06. HRMS(MALDI-TOF):m/z: [[M+H]$^+$calcd for $C_{26}H_{27}N_4O_3$: 443.20777; found: 443.20782.

Photostability

To investigate the photostability of the probe system, the PL intensities ratios of TB-BChE (I_{626}/I_{760}) in PBS solution were monitored by an Edinburgh FS5 fluorescence spectrophotometer, upon continuous irradiation with a 150 W Xe light (575 nm) of the fluorescence spectrophotometer, respectively. The photostability of TB-BChE was demonstrated by plotting I/I_0 versus the irradiation time, where I is the PL intensity ratio of TB-BChE after the irradiation time of t, and I_0 is the PL intensity ratio of TB-BChE before light irradiation.

General procedures for the detection of BChE

Unless otherwise noted, all the spectral measurements were performed in 5 mM phosphate buffer (pH 7.4, containing 0.5% DMSO) according to the following procedure. BChE was dissolved in aqueous solution. The stock solution (1.0 mM) of probe TB-BChE was first prepared in DMSO. 10 μL of TB-BChE stock solution was added to 2 mL PBS followed by addition of different volume of BChE solution. The mixture was incubated at 37 °C, and the reaction solution was transferred to a quartz cell with an optical length of 1 cm for measurement. The excitation and emission slit were set at 5.0 nm and 5.0 nm, respectively.

Determination of the detection limit of TB-BChE toward addition of BChE

Based on the linear fitting in Figure3C, the detection limit (C) is estimated as follows:

$$C = 3\sigma/K$$

Where σ is the standard deviation obtained from three individual fluorescent intensity ratio (I_{626}/I_{760}) of TCFPB-BChE (5 μM) without any BChE and K is the slope obtained after linear fitting the titration curves in Figure 4C.

Inhibition of Enzyme Activity

The inhibitory effect of tacrine on the enzyme activity was determined by the following procedures:

BChE (20 μg/mL) was pre-incubated with different concentrations of tacrine in 2 mL of PBS buffer of pH 7.4 for 30 min then 10 μL of TB-BChE (1.0 mM in DMSO) was added. Fluorescence spectra of the solutions were recorded after incubation for another 30 min. The percent inhibition values corresponding to the presence of different concentrations of tacrine were calculated using the following equation:

$$\text{Inhibition efficiency (\%)} = 100 - [(F_i / F_o) \times 100]$$

where F_o and F_i are the fluorescence intensities obtained for BChE in the absence and presence

of tacrine, respectively.[1]

Kinetic characterization of TB-BChE towards BChE

TB-BChE with different concentrations (0.5, 1, 2, 3, 4, 5, 6, 7, 8, 9, 10, 12, 15, 17 and 20 μM) was hydrolyzed by BChE (10 μg/mL). The reaction was monitored by measuring the fluorescence intensity ratios (I_{626}/I_{760}) for TB-BChE after being incubated in PBS buffer (pH 7.4) for 30 min at 37 °C. the rate of a certain amount of BChE enzyme-catalyzed hydrolysis was plotted with different concentrations of substrate TB-BChE. The kinetic parameters (V_{max} and K_m) for TB-BChE were extrapolated with Origin software based on no less than three independent measurements. The inhibition constants (K_i) for tacrine were obtained by the Dixon plot.

Cell Culture

The Hela cells and LO2 cells were cultured in DMEM (containing 10% heat-inactivated FBS, 100 mg·mL^{-1} penicillin and 100 mg·mL^{-1}streptomycin) at 37 °C in a humidified incubator with 5% CO_2. Before the experiments, the cells were precultured until confluence was reached.

ELISA producre

Collected the cells in a centrifuge tube, and discarded the supernatant after centrifugation. The cell lysate was used to lyse the cells, and then centrifuged at 12,000 g for 30 minutes. Finally, collected the supernatant as the cell lysate to be tested. All the procedures were performed following the instructions of the kit.

a. The slats were taken out of the aluminum foil bag after equilibration at room temperature for 20 minutes.

b. The standard wells and sample wells were set, and then 50 μL of standards of different concentrations were added to the standard wells

c. 10 μL of the sample to be tested were added to the sample well, then 40μL of sample diluent were added.

d. 100 μL horseradish peroxidase (HRP)-labeled detection antibody was added to the standard wells and sample wells, and the reaction wells were sealed with a sealing film, and incubated in 37 °C water bath or incubator for 60 minutes.

e. All the liquid in the wells of the slats were discarded and patted dry with absorbent paper, and then each well was filled with washing liquid, and the washing liquid were removed after standing for 1 minute, and then patted dry with absorbent paper. Repeated washing the plate 5 times.

f. 50 μL of substrates A and B were added to each well, and incubated at 37 °C for 15min in the dark.

g. 50 μL of stop solution was added to each well, and the OD value of each well was measured at 450 nm wavelength within 15 minutes.

h. we used the concentration of the standard product as the abscissa and the corresponding OD value as the ordinate to draw the standard product regression curve, and calculated the concentration value of each sample according to the curve equation.

Fluorescence Imaging in mice and serum

All mice were then injected with 100 μL of PBS containing 50 μM TB-BChE, and the images were

obtained by a small animal optical *in vivo* imaging system (λ_{ex} = 570 nm, Channel I= 600-650 nm, Channel II= 700-780 nm, iso-OMPA= Channel I). Histological analysis was performed on sacrificed mice after the *in vivo* imaging. The liver was immobilized in a 4% paraformaldehyde solution and embedded in paraffin wax. Liver tissue was stained with eosin (H&E) and then examined under a light microscope. The serums were derived from mice in the normal group and nonalcoholic fatty liver group, and the supernatant was centrifuged at 3000 rpm for 30 minutes. Then add TB-BChE (5 μM) 37 °C for 30 minutes, and images were obtained by a small animal optical *in vivo* imaging system.

Computational Methods Details

We used GaussView 5.0[2] and Gaussian 09[3] software for structural visualization and simulation respectively. The structure of the compound is optimized to obtain the minimum energy form. The B3LYP function of DFT is implemented in the current research. For orbitals description, Pople basis set' 6-31G(d) is used for carbon, hydrogen, nitrogen, and oxygen atoms. Generate the highest occupied molecular orbitals (HOMOs) and lowest unoccupied molecular orbitals (LUMOs) to understand the electron density distribution of all compounds.

Molecular docking program

a. We minimized the energy of TB-BChE in the ChemBio3D Ultra 14.0 software, set the Minimum RMS Gradient to 0.001, and then saved the small molecules in mol2 format. Finally, imported the optimized small molecules into AutodockTools-1.5.6 for hydrogenation, charge calculation, charge distribution, set rotation keys, and saved them in the "pdbqt" format.

b. We downloaded the protein structure from the PDB database in the PDB ID, then used Pymol 2.3.0 to remove the protein crystal water, original ligands, etc., and finally imported the protein structure into AutoDocktools (v1.5.6) for hydrogenation, charge calculation, charge distribution, specify the atom type and saved as "pdbqt" format.

c. We used AutoDock Vina1.1.2 for docking. The relevant parameters of 1B41 were set to: center_x = 116.35, center_y = 104.29, center_z = -142.67; Search space: size_x: 126, size_y: 126, size_z: 126 (the spacing of each grid point was 0.375Å), exhaustiveness: 10, other parameters were default settings; 1P0M related parameters were set as: center_x = 138.148, center_y = 122.75, center_z = 38.678; Search space: size_x: 126, size_y: 126, size_z: 126 (the spacing of each grid point was 0.375Å); exhaustiveness: 10, and the rest of the parameters were the default settings.

d. We used PyMOL 2.3.0 and LIGPLOT V 2.2.4 to analyze the interaction mode of the docking results.

Figures and tables

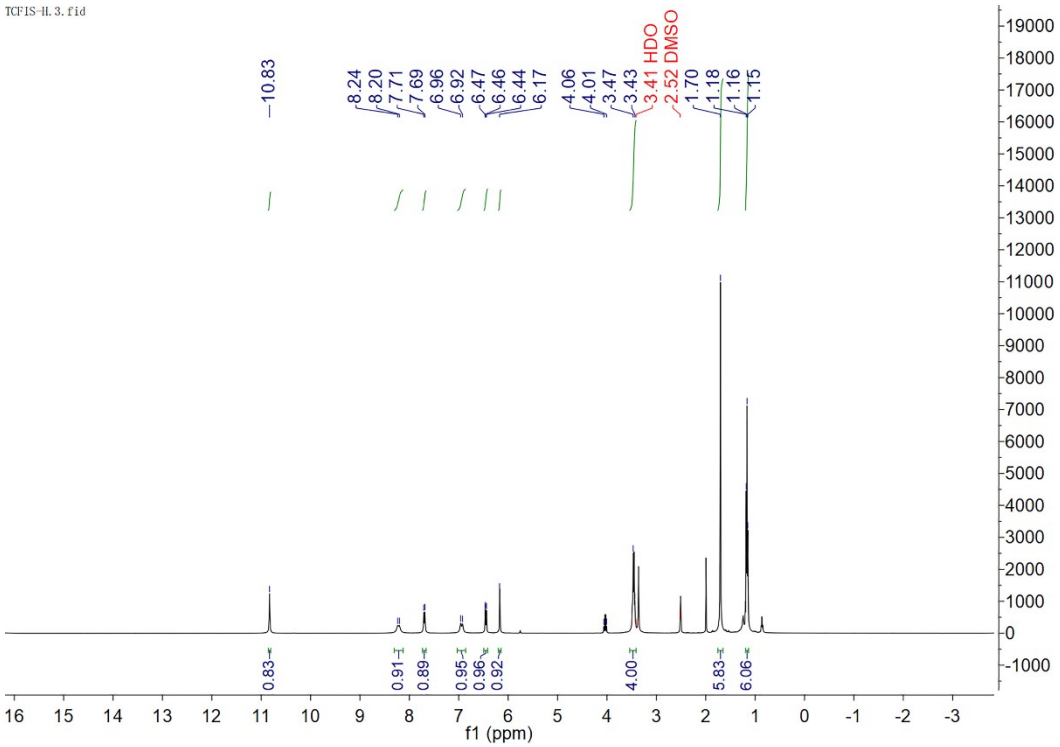

Figure S1. ^{1}H NMR spectrum of **TCFIS** in d_6-DMSO.

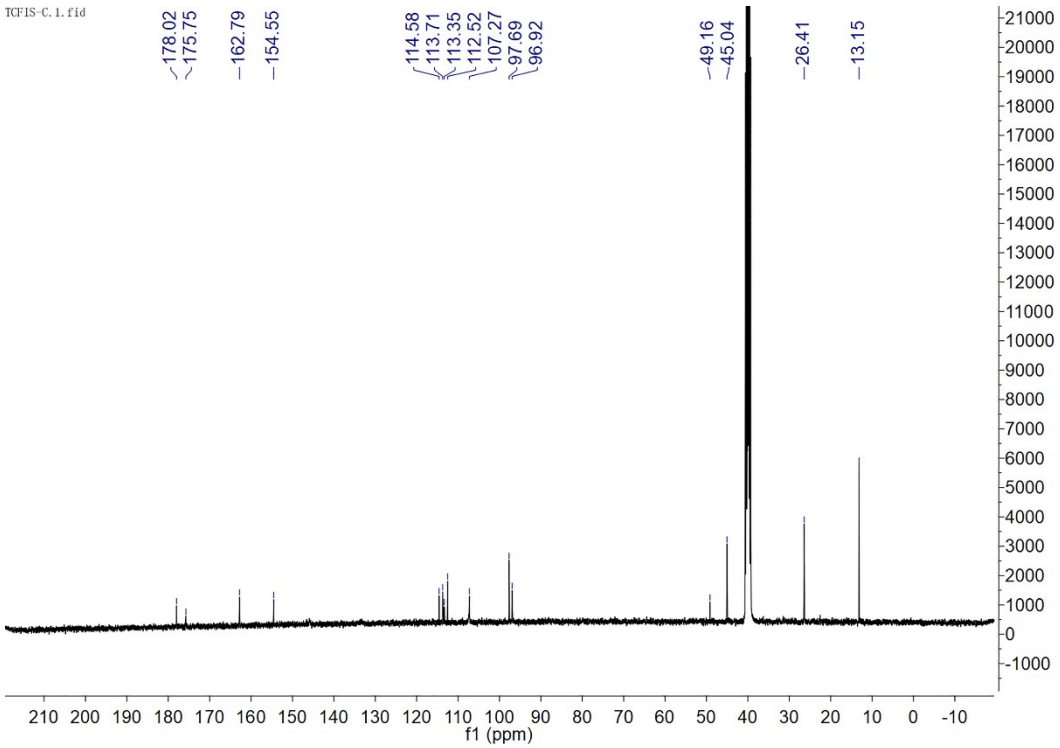

Figure S2. ^{13}C NMR spectrum of **TCFIS** in d_6-DMSO.

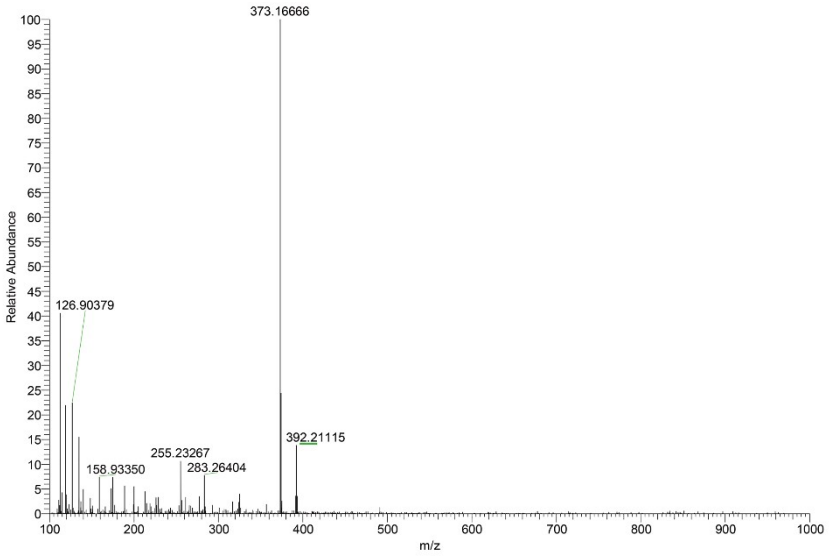

Figure S3. HRMS spectrum of **TCFIS**.

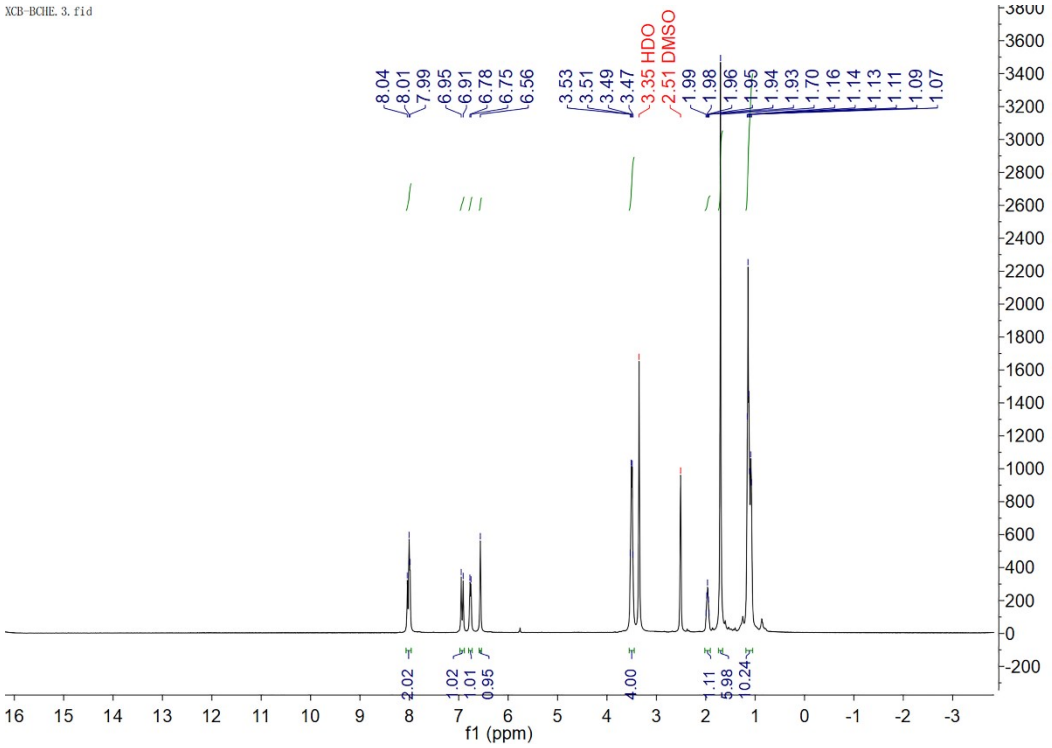

Figure S4. ^{1}H NMR spectrum of **TB-BChE** in d_6-DMSO

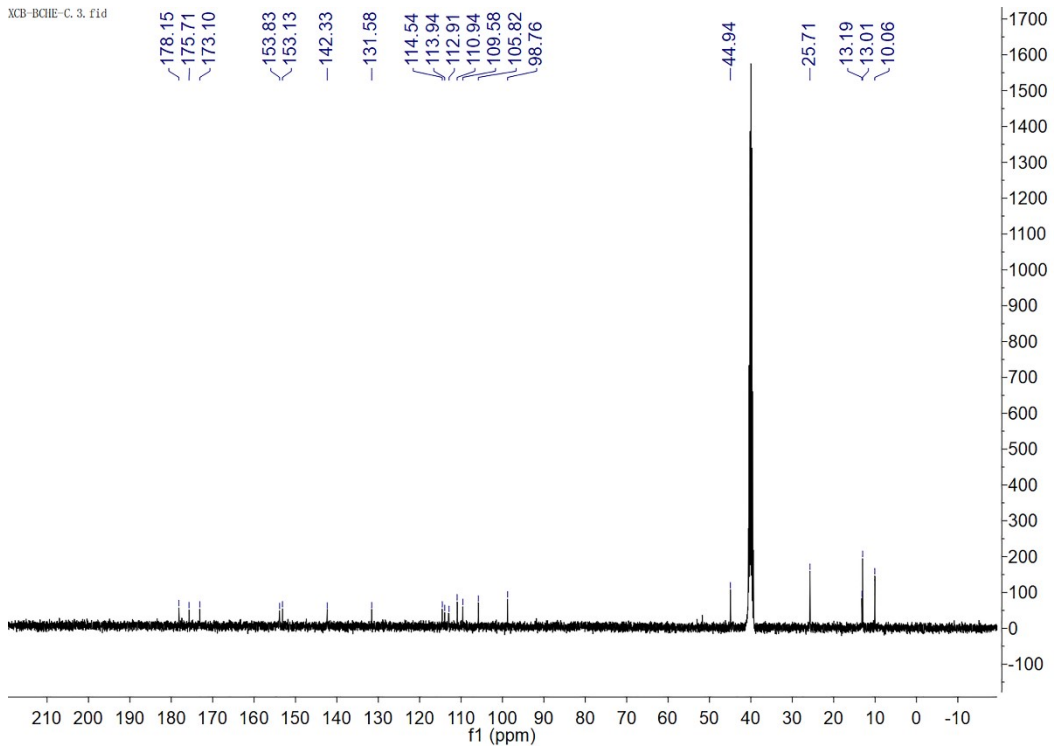

Figure S5. ^{13}C NMR spectrum of **TB-BChE** in d_6-DMSO.

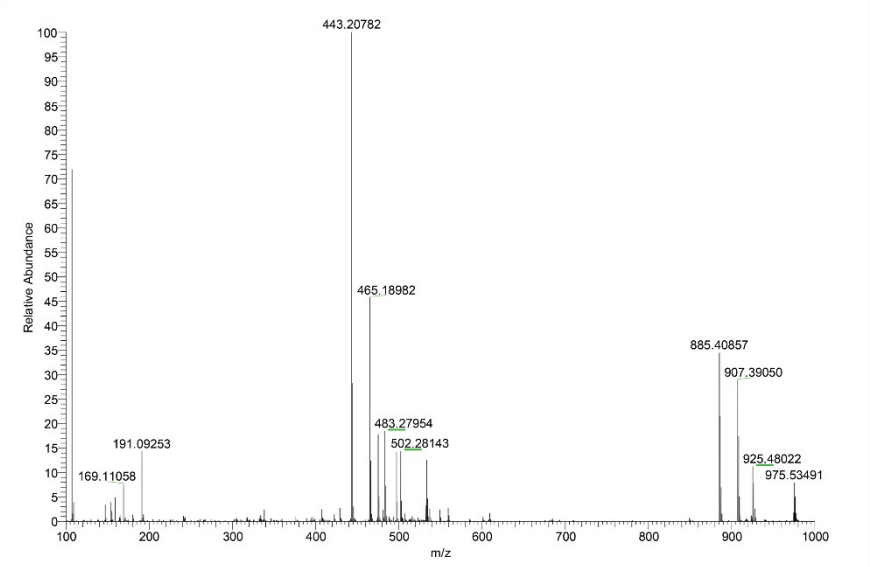

Figure S6. HRMS spectrum of **TB-BChE**.

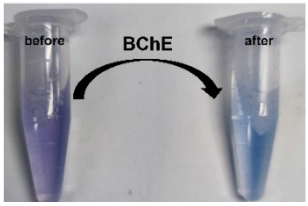

Figure S7. Color change before and after addition BChE to **TB-BChE**, **TB-BChE** = 5 µM, BChE= 90 µg/mL.

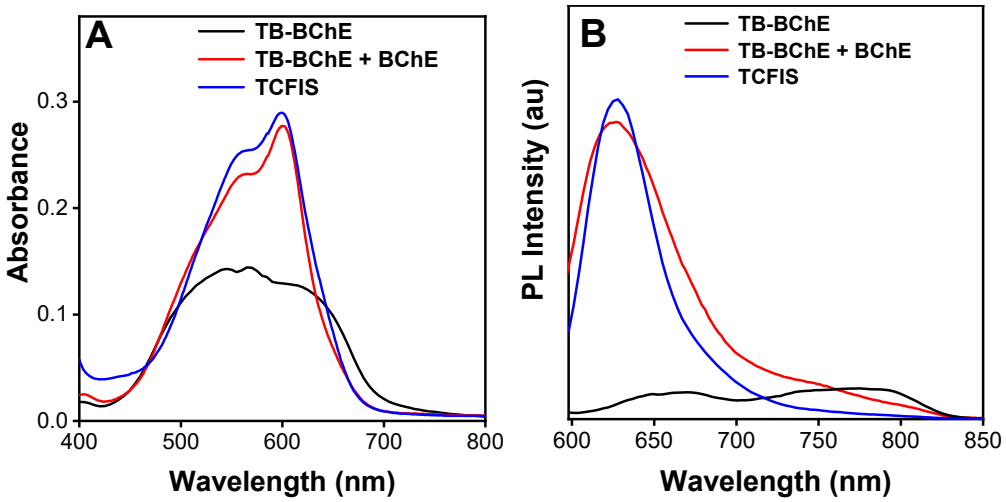

Figure S8. (A) Normalized absorption and Photoluminescence (PL) spectra of **TB-BChE** (5 µM, black), **TCFIS** (5 µM, blue) and (B) **TB-BChE** (5 µM) after incubation with BChE (90 µg/mL, red) at 37°C for 30 min in PBS solution. λ_{ex} = 575 nm.

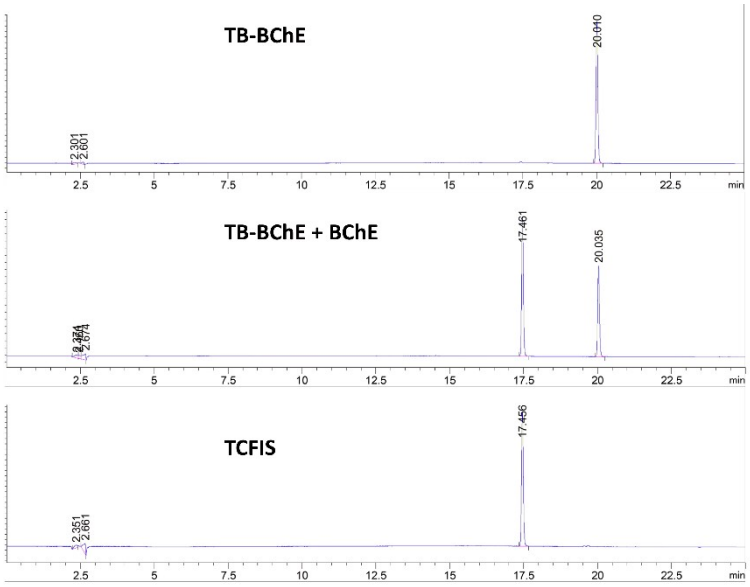

Figure S9. HPLC chromatograms of **TB-BChE** (5 µM), **TB-BChE** with BChE (50 µg/mL), and **TCFIS**. Mobile phase: Acetonitrile/H_2O = 90/10 (v/v).

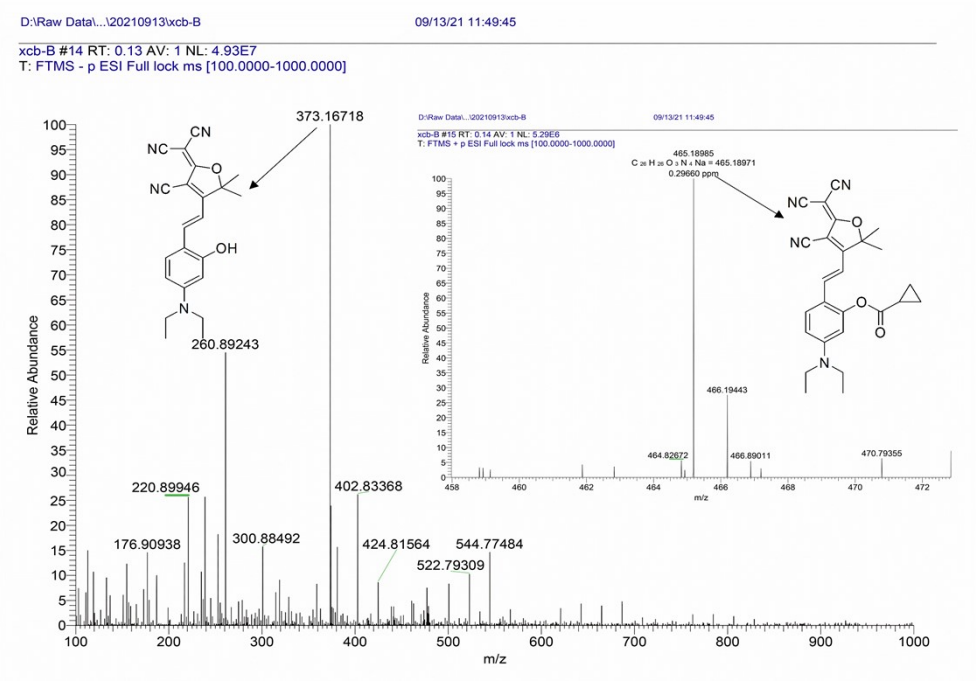

Figure S10. HRMS spectrum of **TB-BChE** after incubation with BChE (90 μg/mL) at 37 °C for 30 min. **TCFIS**([M^+-H] calcd for $C_{22}H_{21}N_4O_2$: 373.16700, found: 373.16718). **TB-BChE**([M+Na]$^+$ calcd for $C_{26}H_{26}N_4O_3Na$: 465.18971, found: 465.18985).

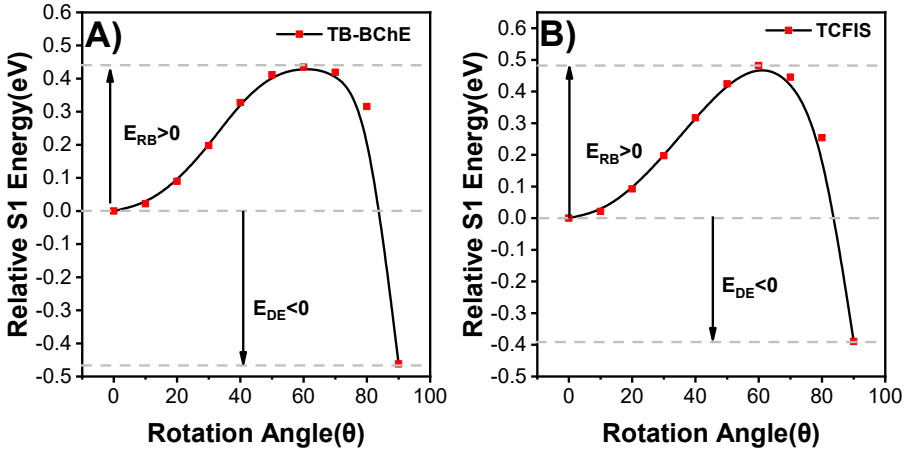

Figure S11. Potential energy surface (PES) curves of TB-BChE (A) and TCFIS (B) at S_1.

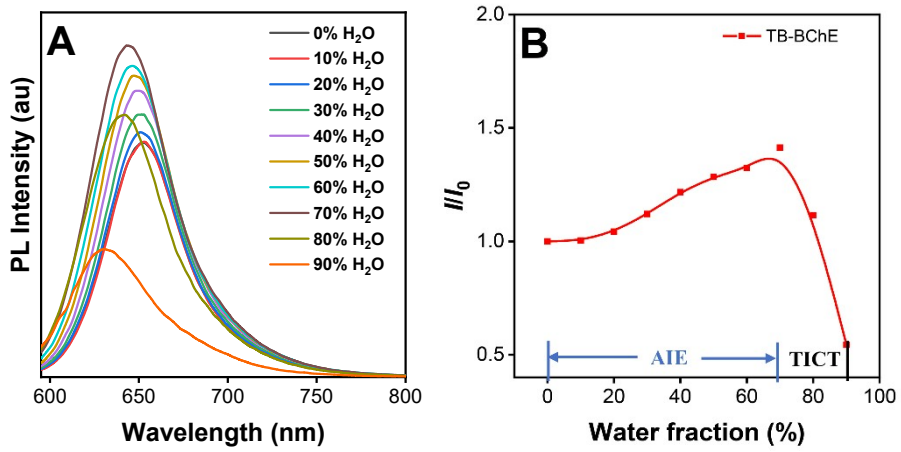

Figure S12. (A) PL spectra of **TB-BChE** (5 μM) in H_2O/THF mixtures with different H_2O fractions. (B) Plot of PL intensity ratios of **TB-BChE** at maximum emission wavelength vs H_2O in the H_2O/THF mixtures. I is the PL intensity of **TB-BChE** after the poor solvent water is added, and I_0 is the PL intensity of **TB-BChE** with 0% water volume fraction. λ_{ex} = 575 nm.

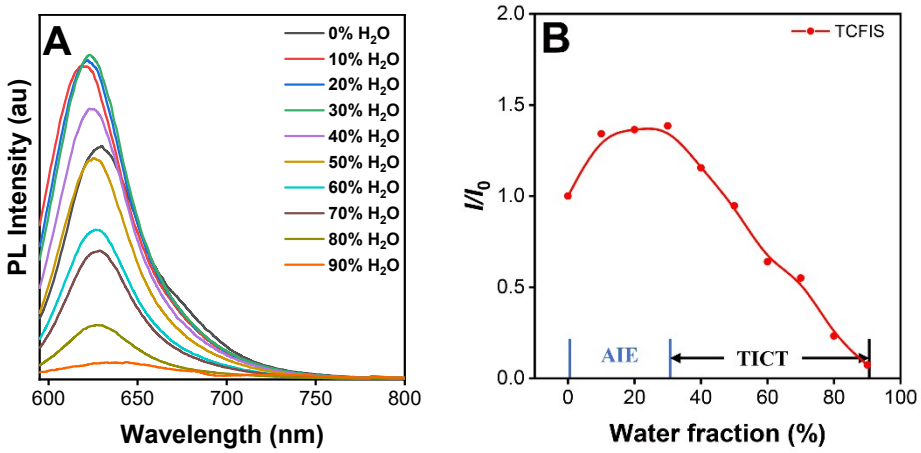

Figure S13. (A) PL spectra of **TCFIS** (5 μM) in H_2O/THF mixtures with different H_2O fractions. (B) Plot of PL intensity ratios of **TCFIS** at maximum emission wavelength vs H_2O in the H_2O/THF mixtures. I is the PL intensity of **TCFIS** after the poor solvent water is added, and I_0 is the PL intensity of **TCFIS** with 0% water volume fraction. λ_{ex} = 575 nm.

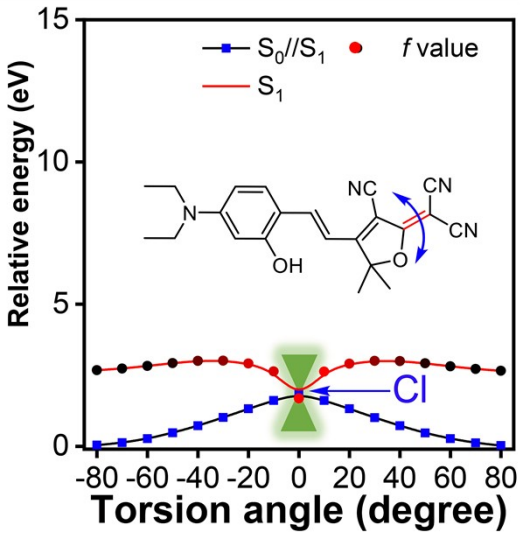

Figure S14. The potential energy surfaces of **TCFIS** geometries in the excited state (S_1) as a function of the torsional angles. S_0//S_1 is the ground state (S_0) projected vertically by S_1.

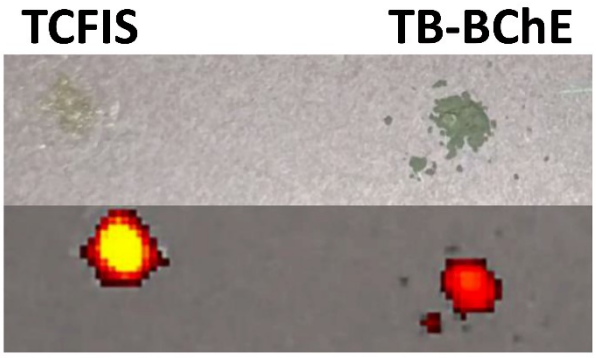

Figure S15. Fluorescence imaging for powder of **TCFIS** and **TB-BChE** under 600 nm light excitation.

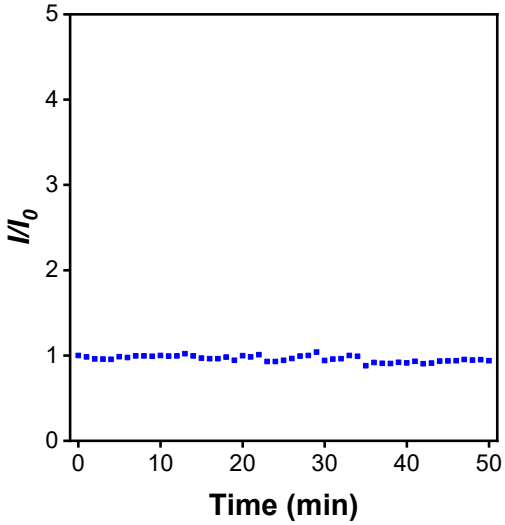

Figure S16. The light stability test of **TB-BChE** in 50 min, **TB-BChE** = 5 μM. λ_{ex} = 575 nm.

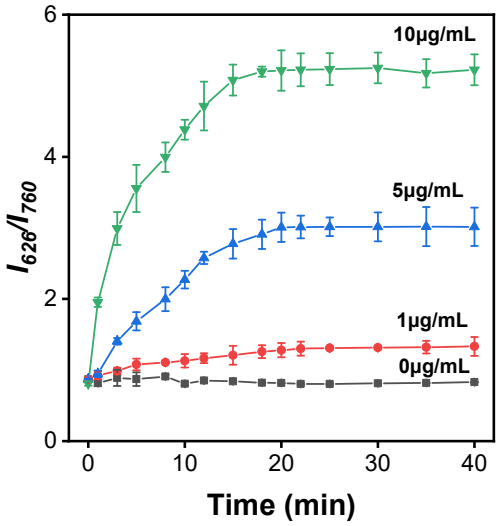

Figure S17. Time-dependent fluorescence intensity ratio (I_{626}/I_{760}) of **TB-BChE** (5 μM) with different concentrations (0, 1, 5 and 10 μg/mL) of BChE. λ_{ex} = 575 nm.

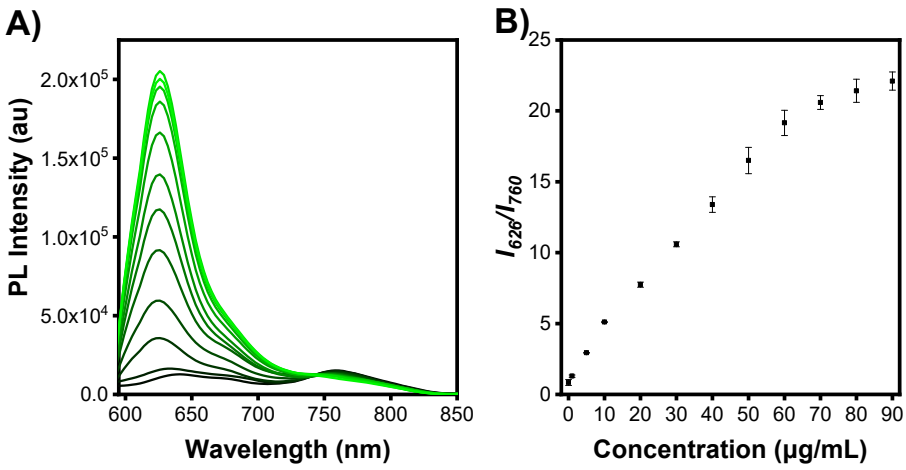

Figure S18. (A) Photoluminescence (PL) spectra of **TB-BChE** (5 μM) after incubation with BChE (0-90 μg/mL) for 30 min. (B) The I_{626}/I_{760} ratios of **TB-BChE** vs. the concentration of BChE (0-90 μg/mL).

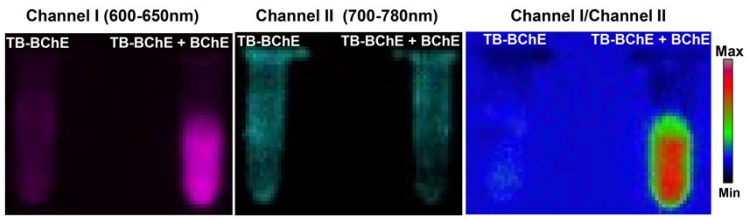

Figure S19. The ratio imaging of the TB-BChE and TB-BChE + BChE. λ_{ex} = 570 nm.

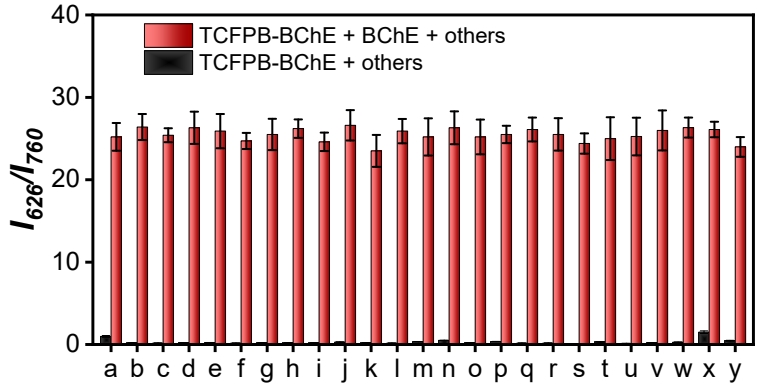

Figure S20. Variations of PL intensity ratios (I_{626}/I_{760}) of **TB-BChE** (5 μM) after incubation with 90 μg/mL BChE and other biologically relevant species; a: AChE (500 μg/mL) ; b: Br^- (500 μM); c: Cl^- (500 μM); d: ClO^- (500 μM); e: Cys (5 mM); f: GSH (5 mM); g: H_2O_2 (500 μM); h:H_2S (500 μM); i: Na_2S_4 (500 μM); j: Hcy (5 mM); k: I^- (500 μM); l: K^+ (500 μM); m: Lactoferrin (500 μg/mL) ; n: Lipase (500 μg/mL); o: lysozyme (500 μg/mL) ; p:Pepsine (500 μg/mL) ; q: Trypsin (500 μg/mL); r: Tyrosinase (500 μg/mL); s :Na^+ (500 μM); t:Ca^{2+} (500 μM); u:Fe^{3+} (500 μM); v:Mg^{2+} (500 μM);w: ATP (5 mM); x: carboxylesterase (20 U/mL); y: Sulfatase (20 U/mL) λ_{ex} = 575 nm.

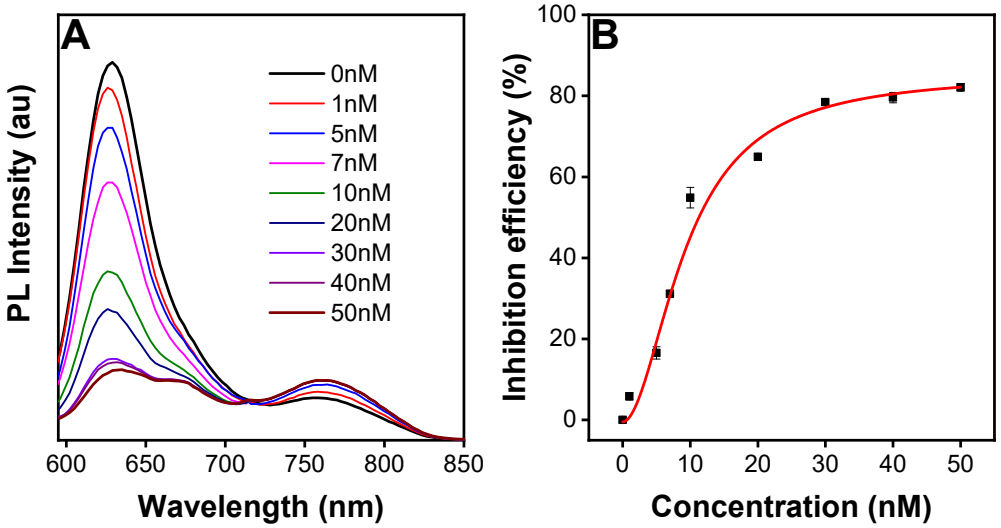

Figure S21. (A)Fluorescence spectra of probe **TB-BChE** with 20 μg/mL BChE pretreated with different concentrations of tacrine ranging from 0 to 50 nM in PBS buffer. (B) Plots of the inhibition efficiency of BChE vs tacrine concentration from 0 to 50 nM. λ_{ex} = 575 nm.

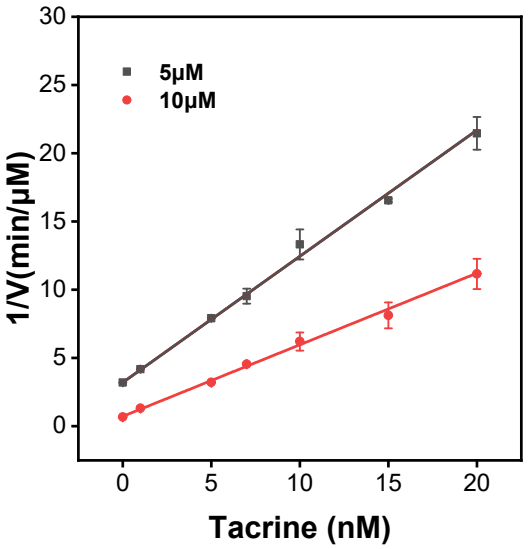

Figure S22. Dixon plots of inhibitory kinetics of tacrine using **TB-BChE** (5 μM and 10 μM) as the substrate.

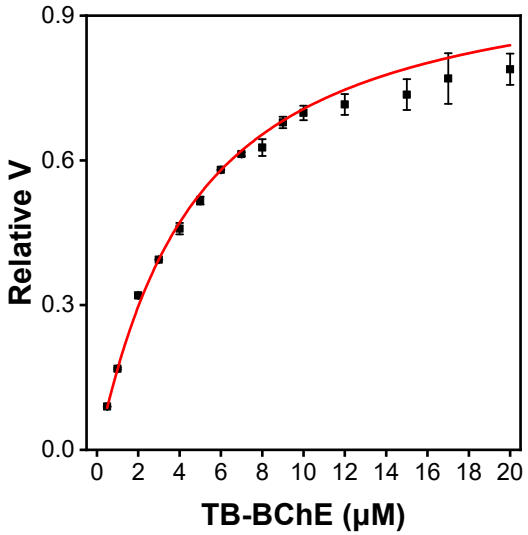

Figure S23. Michaelis-Menten curve for **TB-BChE** reacted with BChE (10 μg/mL).

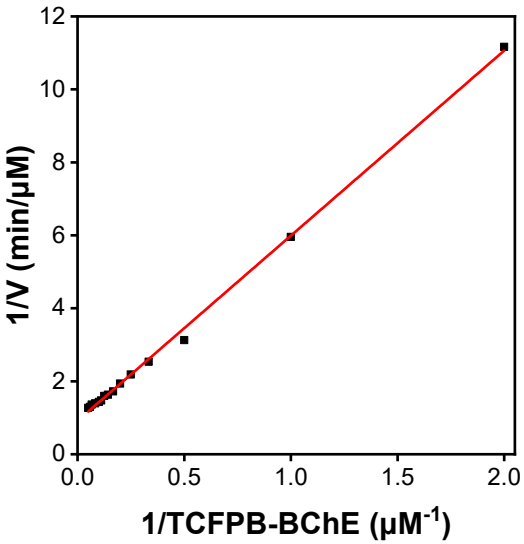

Figure S24. Lineweaver-Burk plot for the enzyme-catalyzed reaction of **TB-BChE**. K_m= 5.53 μM, V_{max}=1.09 μM/min.

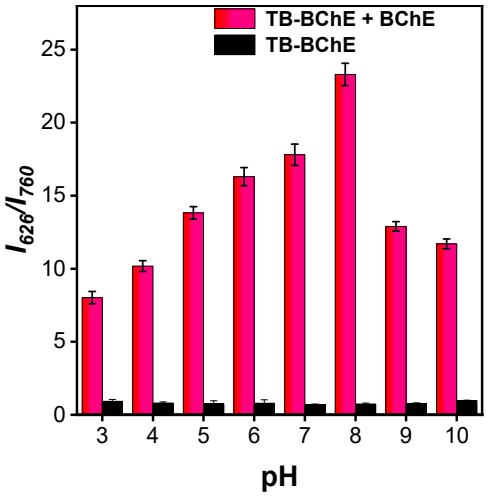

Figure S25. The PL intensity ratios (I_{626}/I_{760}) of **TB-BChE** (5 μM, black bars) and **TB-BChE** (5 μM) + BChE (90 μg/mL, red bars) in different pH buffers. λ_{ex} = 575 nm.

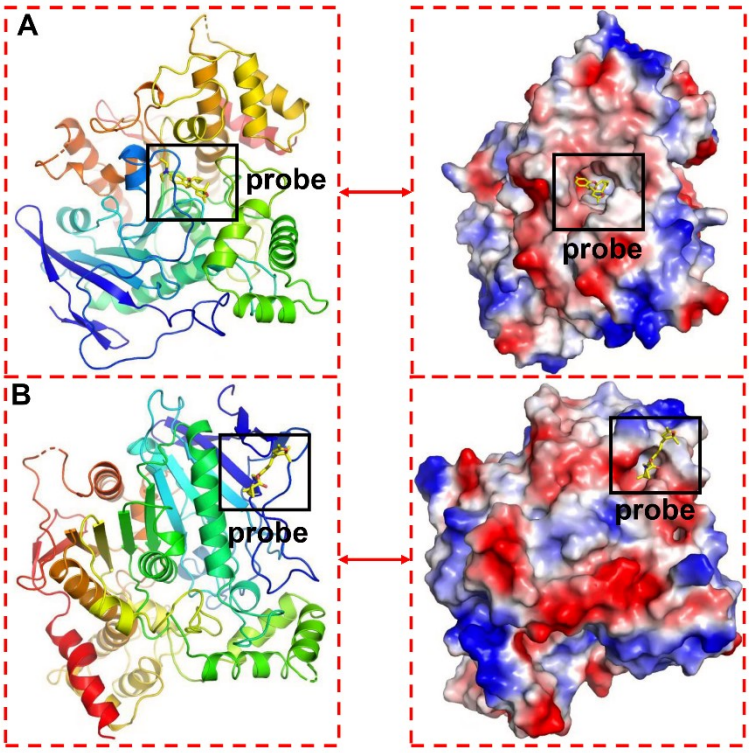

Figure S26. The 3D structure of BChE(A) and AChE(B) containing **TB-BChE**.

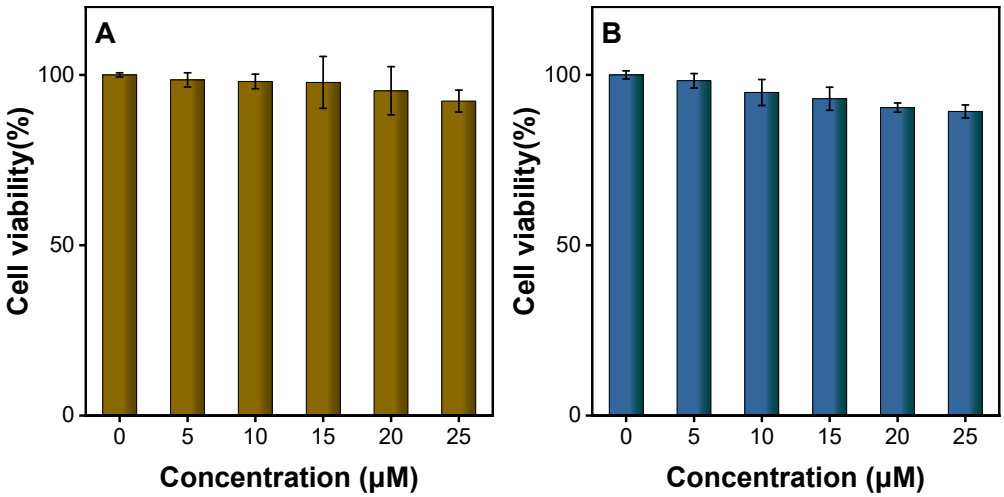

Figure S27. Cell viability of HeLa cells (A) and LO2 cells (B) at varied concentrations of **TB-BChE** by using CCK8 method.

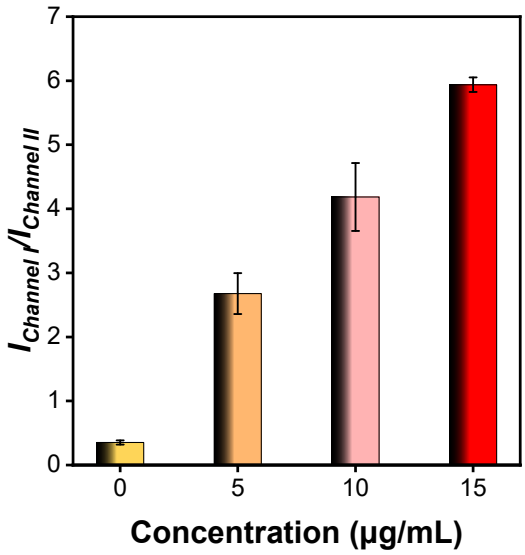

Figure S28. The PL intensity ratio ($I_{channel\ I}/I_{channel\ II}$) of the channel I and channel II in Figure 6.

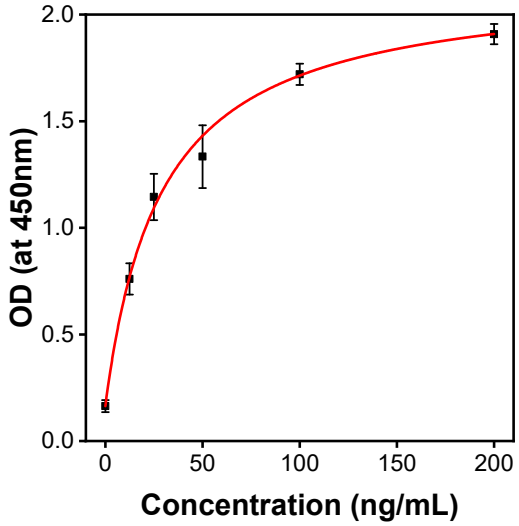

Figure S29. The standard curve of human butyrylcholinesterase (BChE) ELISA Kit, R^2=0.99876.

LO2 cell	Absorbance (at 450nm)	Concentration (ng/mL)
	0.40 ± 0.03	3.75 ± 0.55

Figure S30. The detection data of the Human butyrylcholinesterase (BChE) ELISA Kit in LO2 cells. Each experiment was repeated 4 times. Detection wavelength:450 nm, detection temperature: 26.7 °C.

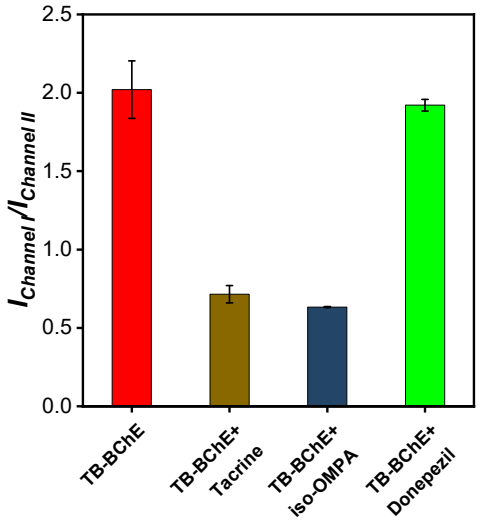

Figure S31. The PL intensity ratio ($I_{channel\ I}/I_{channel\ II}$) of the channel I and channel II in Figure.7.

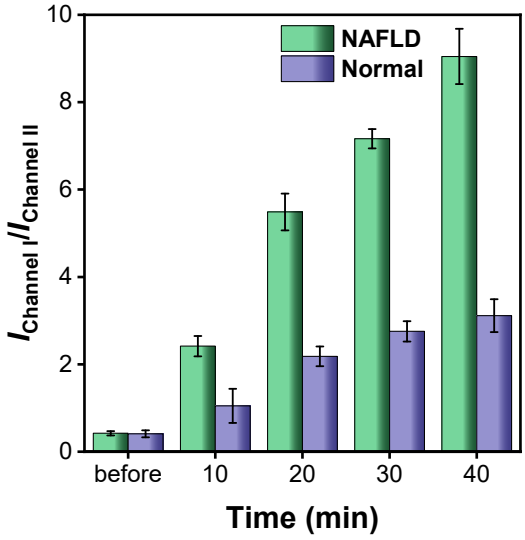

Figure S32. Time-dependent changes of PL intensity ratios in Figure 9.

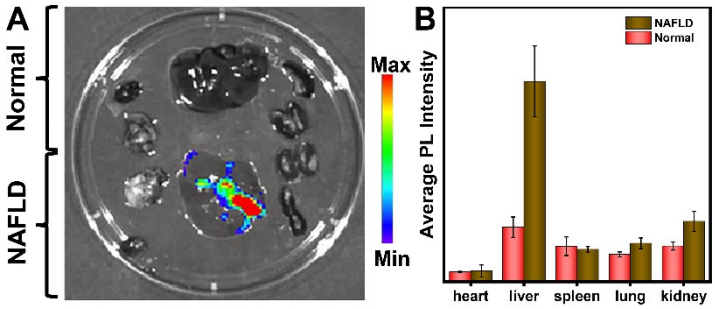

Figure S33. (A) The imaging of the main organs of NAFLD and normal groups. (B) The fluorescence intensity of corresponding organs. λ_{ex} =570 nm, λ_{em} = 600-650 nm.

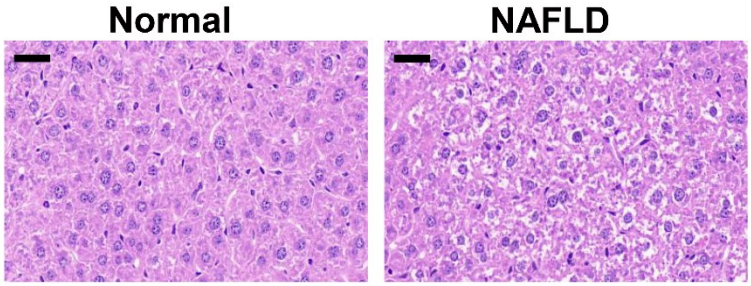

Figure S34. H&E staining of liver tissues (Normal and NAFLD). Scale bar =50 μm.

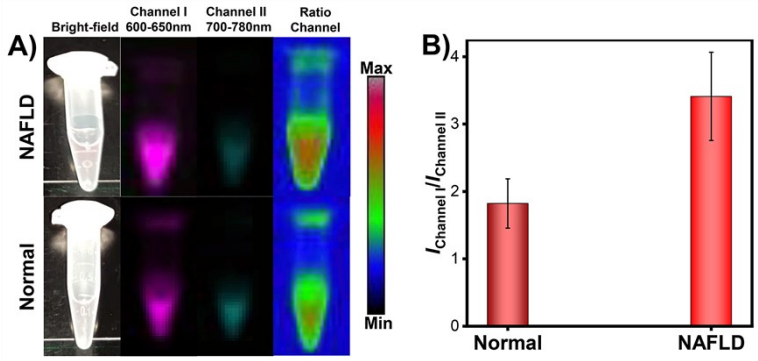

Figure S35. The ratio imaging of the serum for normal and NAFLD group (left) and the corresponding channel I/channel II ratio (right). **TB-BChE**=5 μM, λ_{ex} = 570 nm.

Table S1. Comparison of reported fluorescent probes for BChE detection.

Probe	Response mode	Detection limit	$\lambda_{ex}/\lambda_{em}$ (nm)	Animal disease model	References
Compound 1	on-off (ACQ)	/	355/525	/	*Org. Biomol. Chem.* **2016**, *14*, 8815
BChE-NIRFP	off-on (ACQ)	/	665/705	Alzheimer's disease model	*ACS. Sens*. **2018**, *3*, 2118
BChE-FP	off-on (ACQ)	/	455/515	/	*Chem.Commun*.**2017**,*53*,3952
DCPDA	off-on (ACQ)	60 U/L	-/460	/	*Analyst*. **2019**, *144*, 559
DSC	off-on (ACQ)	1.2 U/L	340/480	/	*Chem.Commun*.**2019**, *55*, 14574
IPAN	off-on (ACQ)	11.7 U/L	545/654	/	*Anal. Chem*. **2020**, *92*, 13405
BChE-NBD	off-on (ACQ)	29 ng/mL	580/628	/	*Sensors and Actuators B: Chemical*. **2021**, *330*,129348
P1	off-on (ACQ)	0.8 U/L	480/528	/	*ACS. Sens*.**2021**, *6*, 1138

CyClC	off-on (ACQ)	3.75 U/L	680/708	/	*Talanta*.**2020**, *219*, 121278
P1	off-on (ACQ)	1.08 μg/mL	600/690	Alzheimer's disease model	*Anal. Chem*. **2021**, *93*, 11337
W1	Ratiometric (ACQ)	0.077 μg/mL	416/446	/	*Dyes Pigm.* **2022**, *197*, 109874.
TB-BChE	**Ratiometric (AIE)**	**39.24 ng/mL**	**575/626**	**Nonalcoholic Fatty Liver**	**This work**

References:

[1] C. Lei, Z. Wang, Z. Nie, H. Deng, H. Hu, Y. Huang and S. Yao, *Anal. Chem*.**2015**, *87*, 1974.

[2] J. Tirado-Rives and W. L. Jorgensen, *J. Chem. Theory. Comput.* 2008, **4**, 297.

[3] T. Mahmood, N. Kosar and K. Ayub, *Tetrahedron*. 2017, **73**, 3521.